Sox10-VENUS BAC Tg mouse: E9.5

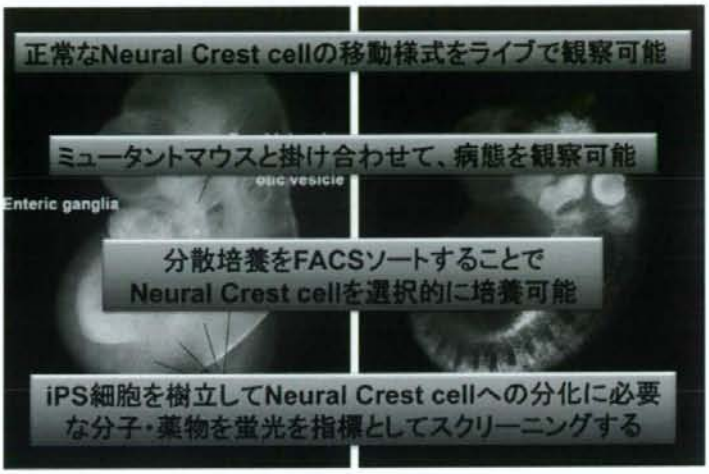

3．小坂　仁

Quantification of PLP mRNA level in cell culture

Design specific primers for Rat *plp*

Isolation of mRNA,
Quantitative RT-PCR

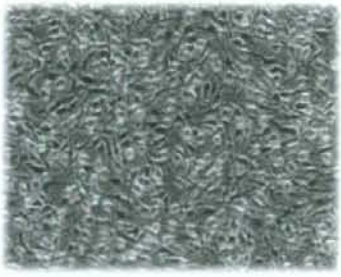

C6 glioma; expressing plp

Inner control;
Hypoxanthine guanine phosphoribosyl transferase

Screening of PLP expression using food chemical library

Incubation period; 48hrs
Cell density; 2.5×10^5/well (9.2cm^2)
Medium; DMEM (low glucose)
Serum; 1% Fetal Bovine Serum
Antibiotics; free

Chemicals extracted from food; ~140
Chemical concentration; 10μM

Supplied by Nippon Suisan Kaisha, Ltd

Example; flavonoids

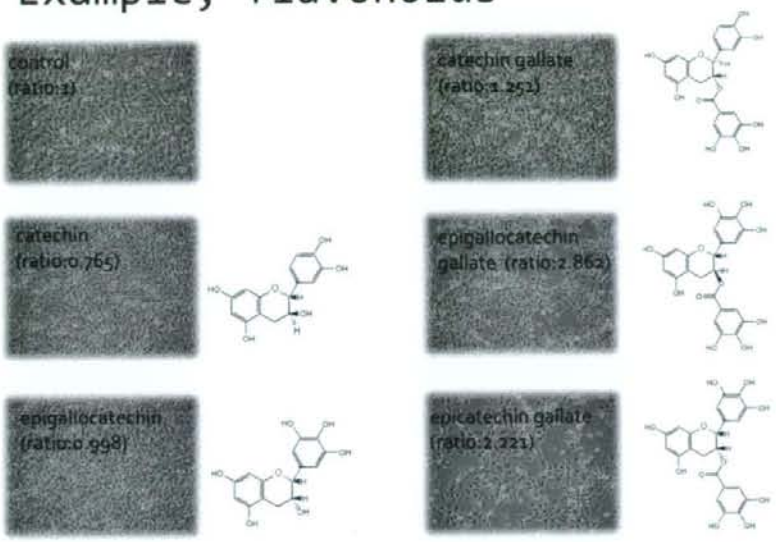

Result (1)

Screening of food chemical library

ratio*	number of chemicals
<0.5	2
≥ 0.5, <0.7	11
≥2.0	15

ratio; plp with chemical/plp without chemical, normalized by HPRT expression

* Mean of duplicate

4．出口貴美子

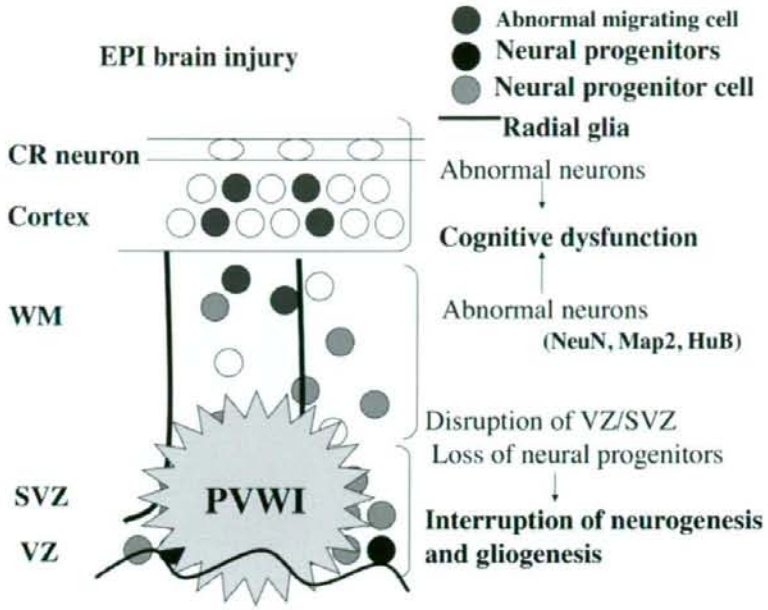

4Y 5Mo female, GA23wks , BBW 523g

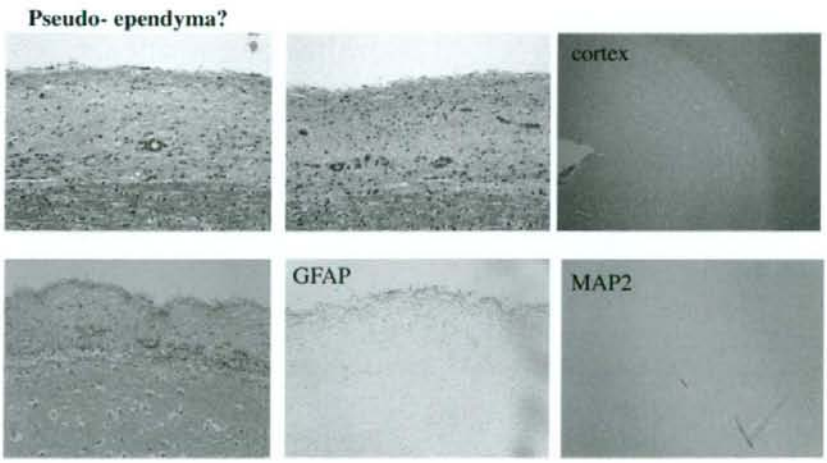

Materials: wild type embrypnic mouse E 16-18

Methods:

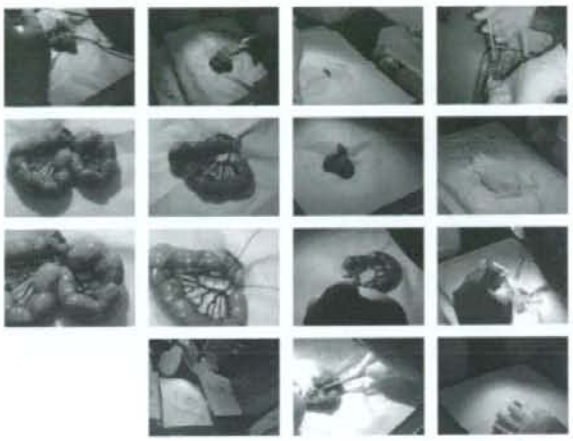

子宮動脈のクリップ

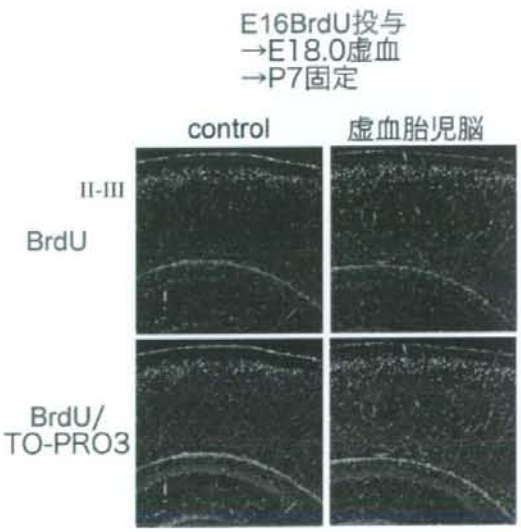

研究成果の刊行に関する一覧表

書籍

著者氏名	論文タイトル名	書籍全体の編集者名	書籍名	出版社名	出版地	出版年	ページ
井上　健	遺伝子治療の最前線	有馬正高、加我牧子、稲垣真澄	小児神経学	診断と治療社	東京	2008	510-511
Osaka, H., Mazaki, E., Okamura, N., Iai, M., Yamada, M., Yamakawa, K., Yamashita, S.	Distinct clinical course of epilepsy with an SCN2A mutation-comparison with SCN1A mutations.	Takao Takahashi, Yukio Fukuyama	Biology of Seizure Susceptibility in Developing Brain. Progress in Epileptic Disorders Series, Vol. 6	John Libbey Eurotext	Montrouge (Paris) France	2008	87-100
小坂　仁	Pelizaeus-Merzbacher 病	小児内科編集部	小児中枢神経疾患の画像診断	東京医学社	東京	2008	484-85
小坂仁、黒澤健司、井合瑞江、山下純正	Pelizaeus-Merzbacher 病の遺伝子診断	辻省次	神経内科	科学評論社	東京	2008	印刷中
森麻子、赤澤智宏	腎疾患・透析・尿路疾患	松浦雅人	臨床病態学	医歯薬出版	東京	2009	未定

雑誌

発表者氏名	論文タイトル名	発表誌名	巻号	ページ	出版年
Deguchi K, Clewing JM, Elizondo LI, Hirano R, Huang C, Choi K, Sloan EA, Lücke T, Marwedel KM, Powell RD, SantaCruz K, Willaime-Morawek S, **Inoue K**, Lou S, Northrop JL, Kanemura Y, van der Kooy D, Okano H, Armstrong DL, Boerkoel CF.	Neurological phenotype of Schimke immuno-osseous dysplasia and neurodevelopmental expression of SMARCAL1.	*J Neuropath Exp Neurol*	67	565-77	2008
Takano K, Nakagawa E, **Inoue K**, Kamada F, Kure S, Goto YI; Japanese Mental Retardation Consortium	A loss-of-function mutation in the *FTSJ1* gene causes nonsyndromic X-linked mental retardation in a Japanese family.	Am J Med Genet B Neuropsychiatr Genet.	147B(4)	479-84	2008
Elizondo LI, Cho KS, Zhang W, Yan J, Huang C, Huang Y, Choi K, Sloan EA, **Deguchi K**, Lou S, Baradaran-Heravi A, Takashima H, Lücke T, Quiocho FA, Boerkoel CF.	Schimke immuno-osseous dysplasia: SMARCAL1 loss-of-function and phenotypic correlation.	J Med Genet.	46(1)	49-59	2009
Goto, A., Wang, Y. L., Kabuta, T., Setsuie, R., **Osaka, H.**, Sawa, A., Ishiura, S., and Wada, K.	Proteomic and histochemical analysis of proteins involved in the dying-back-type of axonal degeneration in the gracile axonal dystrophy (gad) mouse.	Neurochem Int.	*in print*		2008
Saitsu, H., Kato, M., Mizuguchi, T., Hamada, K., **Osaka, H.**, Tohyama, J., Uruno, K., Kumada, S., Nishiyama, K., Nishimura, A., *et al.*	De novo mutations in the gene encoding STXBP1 (MUNC18-1) cause early infantile epileptic encephalopathy.	Nat Genet	40	782-788.	2008
Tanaka, M., Hamano, S., Sakata, H., Adachi, N., Kaga, K., **Osaka, H.**, and	Discrepancy between auditory brainstem responses, auditory	Auris Nasus Larynx	35	404-407.	2008

Kurosawa, K.	steady-state responses, and auditory behavior in two patients with Pelizaeus-Merzbacher disease.				
Liang C, Lee JS, Inn KS, Gack MU, Li Q, Roberts EA, Vergne I, Deretic V, Feng P, **Akazawa C**, Jung JU	Beclin 1-binding UVRAG targets the class C Vps complex to coordinate autophagosome maturation and endocytic trafficking.	Nature Cell Biology	10(7)	776-787	2008
Hashimoto M, Ishii K, Nakamura Y, Watabe K, Kohsaka S, **Akazawa C**	Neuroprotective effect of Sonic hedgehog up-regulated in Schwann cells following sciatic nerve injury.	J Neurochemistry	107(4)	918-927	2008
志村健作、石井邦弥、松尾望、赤澤智宏	BAC トランスジェニックマウス作成法を用いた Neural Crestopathy（神経堤関連疾患）解析の新規モデルマウス作成	順天堂医学	In press		

研究成果の刊行物・別刷（抜粋）

Pelizaeus-Merzbacher 病

小坂　仁
Hitoshi Osaka

key words: Pelizaeus-Merzbacher 病，PLP，ミエリン形成不全

画像診断のポイント

MRI で T2 強調画像ではびまん性の白質の高進号および T1 強調画像で，皮質・白質のコントラストが消失(あるいは極度に低下)していることが特徴的である[1]。

●疾患の概念

Pelizaeus-Merzbacher 病(PMD)は，Pelizaeus(1885，ドイツ人医師)と Merzbacher(1910，ドイツ人病理学者)により最初に記述され，後に Seitelberger(1970)により確立された病理・臨床学的な症候群[2]である。

“白質のミエリン鞘が消失・あるいは極度に低下するがニューロンは保持され，あきらかな脱髄の変化を伴わず，残存したミエリンが斑状の tigroid の像を呈する”ことを特徴とする。その後の遺伝学的な解析により，プロテオリピドプロテイン(proteolipid protein：PLP)の遺伝子異常がこの疾患の原因であることが明らかにされた。ミエリン蛋白の50%以上を占める主要な分子である PLP が，オリゴデンドロサイトに局在するため，中枢神経系に限局した症状を示す。この疾患を疑う臨床症状として，生直後から遅くとも1カ月程度までに眼振に気づかれることが多い。気道感染に際して吸気時喘鳴が聞かれることもある。生後から半年程度までは筋緊張低下の症状を呈する。原始反射の消失が遅れ，Babinski 反射は半年を超えても陽性である。小脳症状としての企図振戦はおもちゃを取ろうとするときの手の動きなどで1歳過ぎには，注意深く観察すると明らかであることが多い。また2歳頃にはアテトーゼ様の異常肢位が発現してくる。このように中枢神経系の，運動，運動制御系，基底核のすべての症状が相次いで出現するのがこの疾患の特徴である。

●どの画像診断法を選択するか

MRI の診断価値が高い。とくに T2 強調像が特徴的である。

●画像所見(図)

生前診断は MRI の出現により，可能となった。その画像はきわめて特徴的である。MRI，T2 強調画像ではびまん性の白質の高進号を示す。T1 強調画像では，皮質・白質のコントラストが消失(あるいは極度に低下)していることが特徴的である。CT 検査では，非特異的な大脳萎縮を認めるのみで診断的な情報は少ない。MRS では *N*-acetylaspartate(NAA)，creatine(Cr)，and myoinositol(MI)の増多を認める[3]。

●画像から鑑別すべき疾患

リソゾーム病では，初期に髄鞘化遅延が目立ったことがあり，紛らわしいことがあるが，MRI 上脱髄(いったん完成化した髄鞘が崩壊している像)を呈する。ことにシアル酸の転送障害による infantile sialic acid disease(ISSD)および Salla 病は非常に PMD に類似した像を呈するが，白質容量低下が PMD よりより著しいことが特徴的とされる。

神奈川県立こども医療センター神経内科　[〒232-8555 横浜市南区六ツ川 2-138-4]
TEL 045-711-2351　FAX 045-721-3324

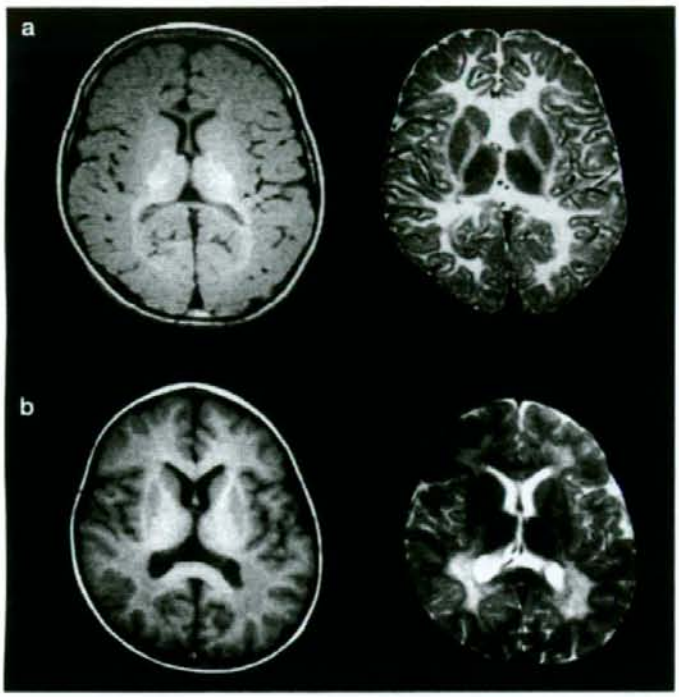

図　症例
a：PLP の重複による PMD，3 歳男児；T1 強調画像では，内包視放線の一部に髄鞘化を認めるが，T2 強調画像では白質の髄鞘化がまったくみられない。
b：異染性白質変性症（metachromatic leukodystrophy）の 3 歳男児；T1 強調画像では，皮質下灰白質に比して，深部灰白質の髄鞘化が不良であり，髄鞘化遅延では説明できない。T2 強調画像でも同様の所見であり，いったん完成した髄鞘が破壊された，脱髄性病変であることを示している。

また，肝脾腫を認めることが本症と異なる（わが国での確定例は文献上 2 例にすぎない）。18q-症候群も，ミエリンの構成蛋白であるミエリン塩基性蛋白遺伝子欠失（常染色体の一方）により髄鞘化遅延の像を呈するが，一方のアリルが正常なため，遅れて髄鞘化が起こり T1 では明らかな異常を認めないことも多い。

●確定診断の方法[4]

ほぼ 5 割の症例で遺伝子重複を認めるので，定量的 PCR 法や FISH 法などにより正常の 2 倍量の PLP の存在を確かめる。2〜3 割の患者では直接塩基配列決定が必要である。なお，この遺伝子は PLP のみならず DM20 もコードしているが，後者の翻訳にはかかわらない領域の変異では非常に臨床症状の軽微な X-linked spastic paraplesia の像を呈する。PLP 変異のキャリア女性では，manifesting carrier として発症する場合がある。PLP 異常によらない PMD 類似の症状を示す症例も 3 割程度存在し，その一部は GJA12 の異常によるものと考えられるがわが国ではまだ報告例がない。また，基底核・小脳萎縮を伴う PMD に類似した一群があり（hypomyelination and atrophy of the basal ganglia and cerebellum），これも PLP とは別の遺伝子の異常に基づくものと考えられる。

文　献
1) van der Knaap MS, Jacob V：Magnetic Resonance of Myelin. Myelination and Myelin Disorders, 3rd ed, Springer, Berlin, pp272-280, 2005
2) Inoue K：PLP1-related inherited dysmyelinating disorders：Pelizaeus-Merzbacher disease and spastic paraplegia type 2. Neurogenetics **6**：1-16, 2005
3) Takanashi J, Inoue K, Tomita M, et al：Brain N-acetylaspartate is elevated in Pelizaeus-Merzbacher disease with PLP1 duplication. Neurology **58**：237-241, 2002
4) Osaka H, Kawanishi C, Inoue K, et al：Pelizaeus-Merzbacher disease：three novel mutations and implication for locus heterogeneity. Ann Neurol **45**：59-64, 1999

nature genetics

De novo mutations in the gene encoding STXBP1 (MUNC18-1) cause early infantile epileptic encephalopathy

Hirotomo Saitsu[1], Mitsuhiro Kato[2], Takeshi Mizuguchi[1], Keisuke Hamada[3], Hitoshi Osaka[4], Jun Tohyama[5], Katsuhisa Uruno[6], Satoko Kumada[7], Kiyomi Nishiyama[1], Akira Nishimura[1], Ippei Okada[1], Yukiko Yoshimura[1], Syu-ichi Hirai[8], Tatsuro Kumada[9], Kiyoshi Hayasaka[2], Atsuo Fukuda[9], Kazuhiro Ogata[3] & Naomichi Matsumoto[1]

© 2008 Nature Publishing Group http://www.nature.com/naturegenetics

Early infantile epileptic encephalopathy with suppression-burst (EIEE), also known as Ohtahara syndrome, is one of the most severe and earliest forms of epilepsy[1]. Using array-based comparative genomic hybridization, we found a *de novo* 2.0-Mb microdeletion at 9q33.3–q34.11 in a girl with EIEE. Mutation analysis of candidate genes mapped to the deletion revealed that four unrelated individuals with EIEE had heterozygous missense mutations in the gene encoding syntaxin binding protein 1 (*STXBP1*). STXBP1 (also known as MUNC18-1) is an evolutionally conserved neuronal Sec1/Munc-18 (SM) protein that is essential in synaptic vesicle release in several species[2–4]. Circular dichroism melting experiments revealed that a mutant form of the protein was significantly thermolabile compared to wild type. Furthermore, binding of the mutant protein to syntaxin was impaired. These findings suggest that haploinsufficiency of *STXBP1* causes EIEE.

EIEE, also known as Ohtahara syndrome[1], is characterized by early onset of tonic spasms, seizure intractability, a characteristic suppression-burst pattern on the electroencephalogram (EEG) and poor outcome with severe psychomotor retardation[5,6]. Many causes have been considered for EIEE. Structural abnormalities of the brain such as hemimegalencephaly, Aicardi syndrome and porencephaly often cause EIEE, but cryptogenic or idiopathic EIEE is found in a subset of individuals, in whom genetic factors could be involved[5,6]. The transition from EIEE to West syndrome, which is characterized by tonic spasms with clustering, arrest of psychomotor development and hypsarrhythmia on the EEG, occurs in 75% of individuals with EIEE[5,6]. A common pathological mechanism linking these two syndromes has been suggested. Consistent with this idea, specific mutations of the *ARX* (aristaless-related homeobox) gene at Xp22.13 have been recently found in male subjects with EIEE and West syndrome[7,8]. In most cryptogenic EIEE cases, however, the genetic cause remains to be elucidated.

Microarray technologies detect genomic copy number alterations, which may be related to disease phenotypes, at a submicroscopic level[9,10]. In a BAC array-based comparative genomic hybridization (aCGH) analysis (containing 4,219 clones with 0.7-Mb resolution for genome-wide analysis) of individuals with mental retardation, we found a microdeletion at 9q33.3–q34.11 in a girl with EIEE (subject 1) (**Fig. 1a**). The deletion was 2.0 Mb in size and was confirmed by fluorescent *in situ* hybridization (FISH) analysis on the subject's chromosomes (**Fig. 1b**), whereas no deletion was found in her parents (data not shown).

More than forty genes mapped within the deletion (**Fig. 1b**). Among them, the gene encoding syntaxin binding protein 1 (STXBP1, also known as MUNC18-1) was of interest because mouse *Stxbp1* has been shown to be essential for synaptic vesicle release[2], and it is specifically expressed in the brains of rodents and humans[11,12]. We screened for *STXBP1* mutations in 13 unrelated individuals with EIEE. A total of four heterozygous missense mutations were found in three males and a female (**Table 1**): 251T>A (V84D) (subject 11), 539G>A (C180Y) (subject 6), 1328T>G (M443R) (subject 7) and 1631G>A (G544D) (subject 3) (**Fig. 2**). All mutations occurred at evolutionary conserved amino acids (**Fig. 2**). Parental DNAs were available except for subject 3, whose father was deceased. *STXBP1* mutations in subjects 6, 7 and 11 were *de novo* events, as their parents did not possess the same nucleotide

[1]Department of Human Genetics, Yokohama City University Graduate School of Medicine, 3-9 Fukuura, Kanazawa-ku, Yokohama 236-0004, Japan. [2]Department of Pediatrics, Yamagata University School of Medicine, 2-2-2 Iida-nishi, Yamagata 990-9585, Japan. [3]Department of Biochemistry, Yokohama City University Graduate School of Medicine, 3-9 Fukuura, Kanazawa-ku, Yokohama 236-0004, Japan. [4]Division of Neurology, Clinical Research Institute, Kanagawa Children's Medical Center, 2-138-4 Mutsukawa, Minami-ku, Yokohama 232-8555, Japan. [5]Department of Pediatrics, Epilepsy Center, Nishi-Niigata Chuo National Hospital, 1-14-1 Masago, Nishi-ku, Niigata 950-2085, Japan. [6]Epilepsy Center, Yamagata National Hospital, 126-2 Gyosai, Yamagata 990-0876, Japan. [7]Department of Neuropediatrics, Tokyo Metropolitan Neurological Hospital, 2-6-1 Musashidai, Fuchu 183-0042, Japan. [8]Department of Molecular Biology, Yokohama City University Graduate School of Medicine, 3-9 Fukuura, Kanazawa-ku, Yokohama 236-0004, Japan. [9]Department of Physiology, Hamamatsu University School of Medicine, 1-20-1 Handayama, Hamamatsu 431-3192, Japan. Correspondence should be addressed to H.S. (hsaitsu@yokohama-cu.ac.jp) or N.M. (naomat@yokohama-cu.ac.jp).

Received 8 February; accepted 17 March; published online 11 May 2008; doi:10.1038/ng.150

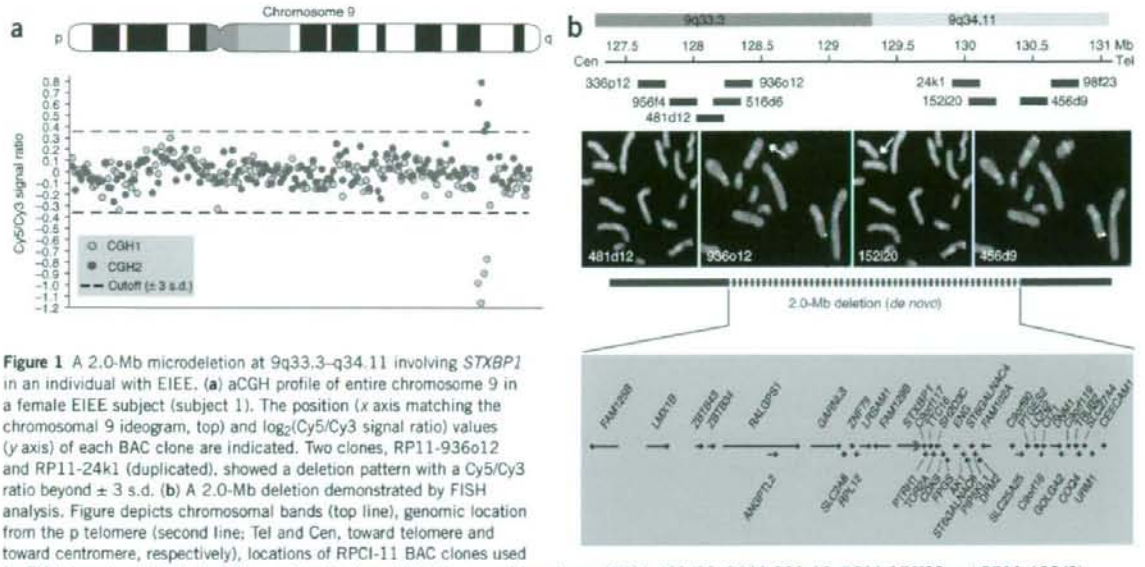

Figure 1 A 2.0-Mb microdeletion at 9q33.3–q34.11 involving *STXBP1* in an individual with EIEE. (**a**) aCGH profile of entire chromosome 9 in a female EIEE subject (subject 1). The position (*x* axis matching the chromosomal 9 ideogram, top) and $\log_2$(Cy5/Cy3 signal ratio) values (*y* axis) of each BAC clone are indicated. Two clones, RP11-936o12 and RP11-24k1 (duplicated), showed a deletion pattern with a Cy5/Cy3 ratio beyond ± 3 s.d. (**b**) A 2.0-Mb deletion demonstrated by FISH analysis. Figure depicts chromosomal bands (top line), genomic location from the p telomere (second line; Tel and Cen, toward telomere and toward centromere, respectively), locations of RPCI-11 BAC clones used for FISH (purple, deleted; dark blue, not deleted), and FISH images of four clones (RP11-481d12, RP11-936o12, RP11-152i20 and RP11-456d9) hybridized to the subject's chromosomes. White arrows, deletion. A total of 41 RefSeq genes, including *STXBP1*, are mapped within the 2.0-Mb region (bottom).

changes. Parentage was confirmed using several microsatellite markers (data not shown). All of the nucleotide changes were absent in 250 healthy Japanese controls (500 chromosomes).

Clinical features of the subjects with EIEE having *STXBP1* defects are summarized in **Table 1** (see also **Supplementary Note** online). Subject 1 has been previously described[13]. Brain magnetic resonance imaging (MRI) did not detect any apparent structural anomalies or hippocampal abnormalities, but showed some atrophy (**Fig. 3a–e**). Three subjects (subjects 1, 6 and 7) showed delayed myelination or hypomyelination[13] (**Fig. 3b–d**). Suppression-burst patterns on EEGs were recognized in all subjects (**Fig. 3f**). Tonic spasms developed 10 d to 3 months after birth (**Supplementary Video 1** online for subject 7). In four subjects (subjects 1, 6, 7 and 11), transition from EIEE to West syndrome with hypsarrhythmia on the EEG occurred (**Fig. 3g**). In subject 3, the EEG at 35 years of age showed independent or synchronized focal spikes, or sharp waves in the bilateral frontal area (**Fig. 3h**). We did not observe any differences of clinical symptoms between mutation-positive and mutation-negative subjects.

All four mutant proteins have amino acid replacements in the hydrophobic core of STXBP1 that would be considered to destabilize their folding architecture; in particular, three of the mutants (V84D, G544D and M443R) have replaced the wild-type (WT) residues with charged residues that would be predicted to severely disrupt the conformation of STXBP1 (**Fig. 4a**)[14]. Thus, the mutated proteins are likely to be structurally unstable. To examine properties of the mutant STXBP1 proteins, we purified recombinant WT and mutant proteins using the GST-tag method. Circular dichroism spectra revealed that the helical content of the C180Y mutant was slightly lower (39%) than that of WT (43%), suggesting that the mutation destabilized the secondary structure of STXBP1 (**Fig. 4b**)[15]. Moreover, circular-dichroism melting experiments showed that the C180Y mutation lowered the thermostability of STXBP1. The obtained melting (transition midpoint) temperature (T_m) of the C180Y mutant was about 11 °C lower than that of the WT (49.53 ± 0.03 °C for the WT and the 38.54 ± 0.03 °C for the C180Y mutant) (**Fig. 4c**). As the T_m of the C180Y mutant is close to the physiological temperature of human body, its functional activity is less likely to be retained in human brain. Although gel filtration experiments showed that the purified C180Y mutant existed as a monomer as did the wild-type (data not shown), other STXBP1 mutants (V84D, G544D and M443R) easily tended to form aggregates, and thus we did not obtain sufficient amounts of these proteins for biophysical analyses. Furthermore, transient expression in Neuroblastoma 2A cells revealed that all of the mutant STXBP1 proteins (V84D, C180Y, M443R and G544D), but not WT-STXBP1, tended to aggregate (**Supplementary Fig. 1** online), suggesting that all of the mutant proteins are structurally unstable.

It has been reported that Stxbp1 regulates synaptic vesicle release, at least in part, by binding to syntaxin 1A (Stx1a) as well as to the SNARE complex directly[16,17]. Stxbp1 binds to Stx1a in two different ways: binding to a closed form of Stx1a and binding to the N terminus of an open form of Stx1a compatible with SNARE complex formation[16–18]. The interaction with the N terminus of open-form Stx1a is important in synaptic vesicle release, whereas interaction with closed-form Stx1a is involved in synaptic vesicle docking[16–19]. Thus, we examined whether the C180Y mutant could bind to the closed and/or open forms of STX1A, using the GST pull-down assay at 4 °C. WT STXBP1 bound to both closed and open forms of GST-STX1A at comparable levels; the C180Y mutant showed decreased binding to both forms of GST-STX1A, particularly the open one, compared to WT STXBP1 (**Fig. 4d,e**). Thus, we would expect synaptic vesicle release to be greatly impaired in the individual with the C180Y substitution.

We identified one complete deletion and four missense mutations of *STXBP1* in individuals with EIEE (three male and two female). STXBP1 is a member of the evolutionary conserved SM gene family that acts at specific steps of intracellular membrane transport[20,21]. In

© 2008 Nature Publishing Group http://www.nature.com/naturegenetics

© 2008 Nature Publishing Group http://www.nature.com/naturegenetics

Table 1 Summary of clinical features of EIEE subjects with *STXBP1* defects

Subject	Sex	*STXBP1* defect	Initial symptoms	Age at onset of spasms	Initial EEG	Age at transition to West syndrome	Response to therapy; frequency of medication	Development	Neurological examination	MRI	Ref.
1	F	Deletion	Tonic seizure and oral automatism	2 mo	Suppression-burst	3 mo	Seizure free from 5 mo after TRH injection	Poor visual attention No rolling over	Profound MR Hypotonic quadriplegia	Cortical atrophy Diffuse hypomyelination Thin corpus callosum (at 12 mo)	Ref. 13
3	M	1631G>A (G544D)	Blinking	10 d	Suppression-burst	–	Seizure free from 3 mo	Walking at 7 yr A few words Feeds self	Profound MR Mild spastic diplegia	Normal (at 37 yr)	–
6	M	539G>A (C180Y)	Tonic seizure with blinking	3 mo	Suppression-burst	4 mo	Intractable; daily	Weak eye pursuit No smile No head control	Profound MR Severe spastic quadriplegia	Mild atrophic change Delayed myelination (at 3 mo)	–
7	F	1328T>G (M443R)	Upward gazing and tonic seizure	2 mo	Suppression-burst	4 mo	Intractable; hourly TRH injection temporarily effective	No head control No words	Profound MR Mild spastic quadriplegia	Mild atrophic change Delayed myelination (at 13 mo)	–
11	M	251T>A (V84D)	Spasms and tonic-clonic seizure	2 mo	Suppression-burst	9 mo	Intractable, daily	No head control No words	Profound MR Severe hypotonic quadriplegia Choreoathetosis	Mild atrophic change of frontal lobe (at 8 yr)	–

MR, mental retardation; TRH, thyrotropin-releasing hormone; mo, month(s); yr, year(s).

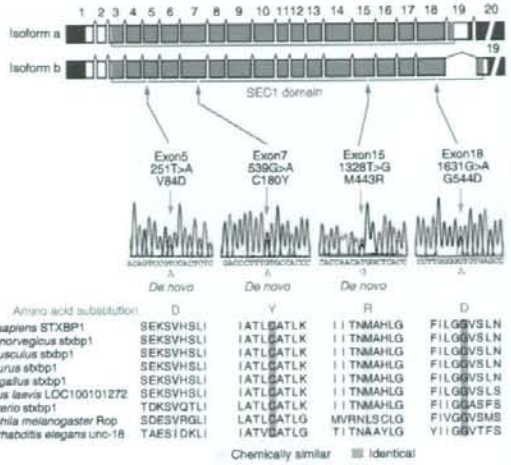

Figure 2 Heterozygous mutations of *STXBP1* found in individuals with EIEE. Schematic representation of *STXBP1* consisting of 20 exons (rectangles). There are two isoforms: isoform a (GenBank accession number, NM_003165) with exon 19, and isoform b (NM_001032221) without exon 19 of isoform a. UTR, coding region, and SEC1 domain are dark blue, white and sky blue, respectively. All of the missense mutations occurred at evolutionary conserved amino acids in the SEC1 domain. Three mutations were confirmed as *de novo*; the other could not be confirmed, as the father was deceased. Homologous sequences were aligned using the CLUSTALW web site.

mammalian exocytosis, the vesicular SNARE protein, VAMP2 (synaptobrevin2), and the target membrane SNARE proteins, Syntaxin-1 and SNAP25, constitute the core fusion machinery that brings two membranes into close apposition to fuse[17,22]. Stxbp1 was first identified as a protein interacting with Syntaxin-1A (ref. 23), and its null mutation leads to complete loss of neurotransmitter secretion from synaptic vesicles throughout development in mice, though seizures have never been described[2]. Thus, STXBP1 is very likely to play a central role for synaptic vesicle release in coordination with SNARE proteins. Knowledge of the genetic bases of epilepsies is increasing rapidly, but most genes associated with epilepsy syndromes are ion channel genes[24]. A mutation in the gene encoding synapsin I, a synaptic vesicle protein thought to regulate the kinetics of neurotransmitter release during priming of synaptic vesicles, has been identified in a family with X-linked epilepsy and learning difficulties[25]. This is the second report implicating aberrations in genes involved in synaptic vesicle release in epilepsy.

All four of the mutant STXBP1 proteins seemed to be structurally unstable because of their amino acid replacements in the hydrophobic core[14]. In fact, in the case of the C180Y mutant STXBP1, its thermal instability occurred near body temperature, and its impaired binding to the open form of STX1A implies that the mutation is hypomorphic or amorphic with regard to synaptic vesicle release. It is also known that *Stxbp1* heterozygous knockout mice show impaired synaptic function owing to reduced size and replenishment rate of readily releasable vesicles[26], suggesting that the functionally impaired STXBP1 may affect synaptic function in the human brain. Considering that the microdeletion involving *STXBP1* also resulted in EIEE, haploinsufficiency of *STXBP1* is the likely cause of EIEE.

It is unknown how haploinsufficiency of *STXBP1* leads to EIEE. EIEE is commonly associated with various structural brain

© 2008 Nature Publishing Group http://www.nature.com/naturegenetics

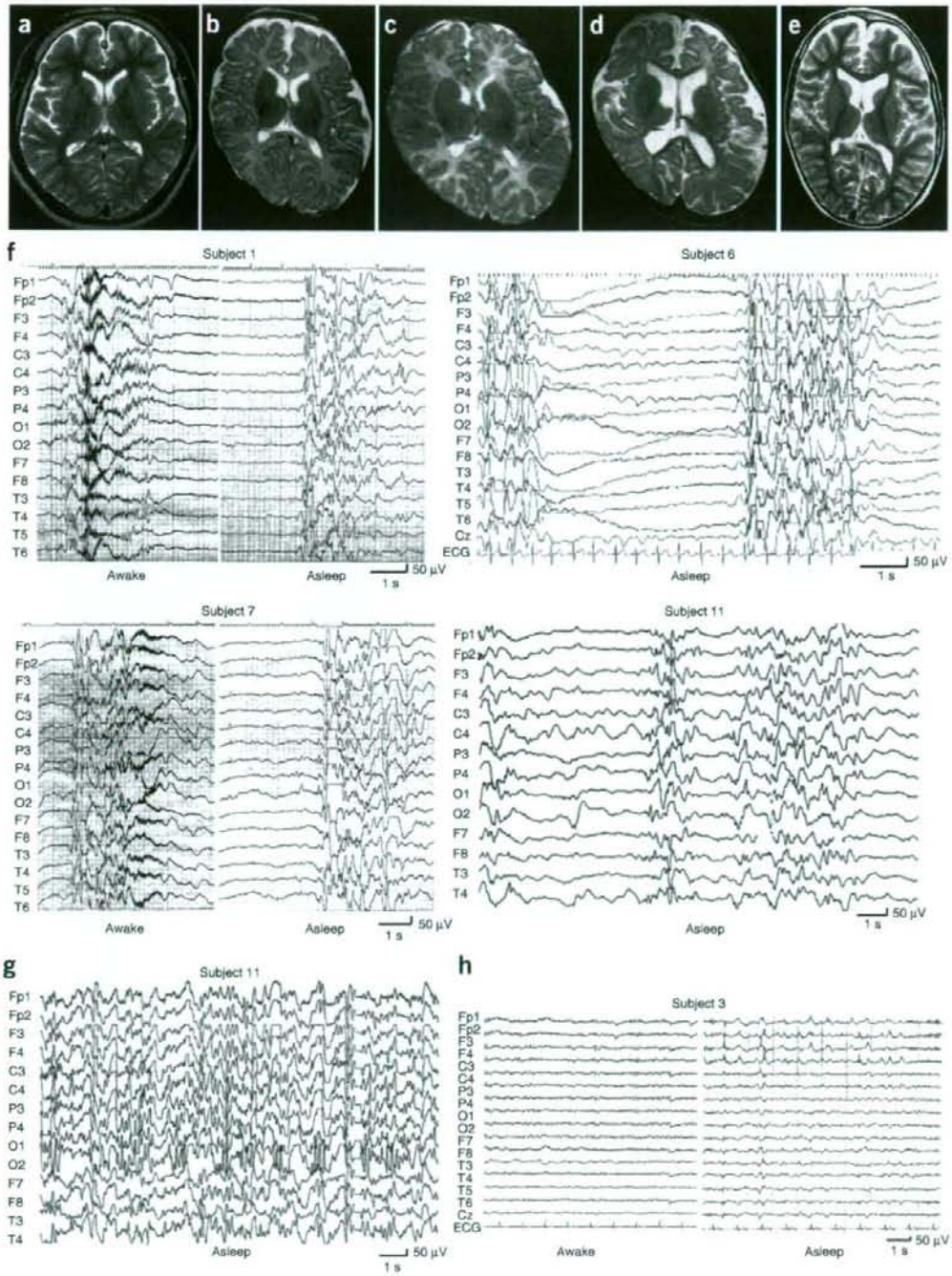

Figure 3 Brain MRI and EEG of subjects with EIEE having *STXBP1* defects. (**a**–**e**) Brain MRI T2-weighted axial images through the basal ganglia showing normal brain structure in the subjects with *STXBP1* mutation (**a**, subject 3 at age of 37 years of age; **b**, subject 6 at 3 months; **c**, subject 7 at 3 months; **d**, subject 7 at 13 months; **e**, subject 11 at 8 years). (**f**) Suppression-burst on interictal EEG of subjects 1 (at age 2 months), 6 (at 3 months), 7 (at 2 months) and 11 (at 3 months). High-voltage bursts alternate with almost flat suppression phases at an approximately regular rate in both awake and asleep states. (**g**) Hypsarrhythmia on interictal EEG of the subject 11 at age of 8 years. Transition from EIEE to West syndrome was recognized at age of 9 months. (**h**) EEG of the 35-year-old subject 3, showing focal spikes or sharp waves in the bilateral frontal area during sleep.

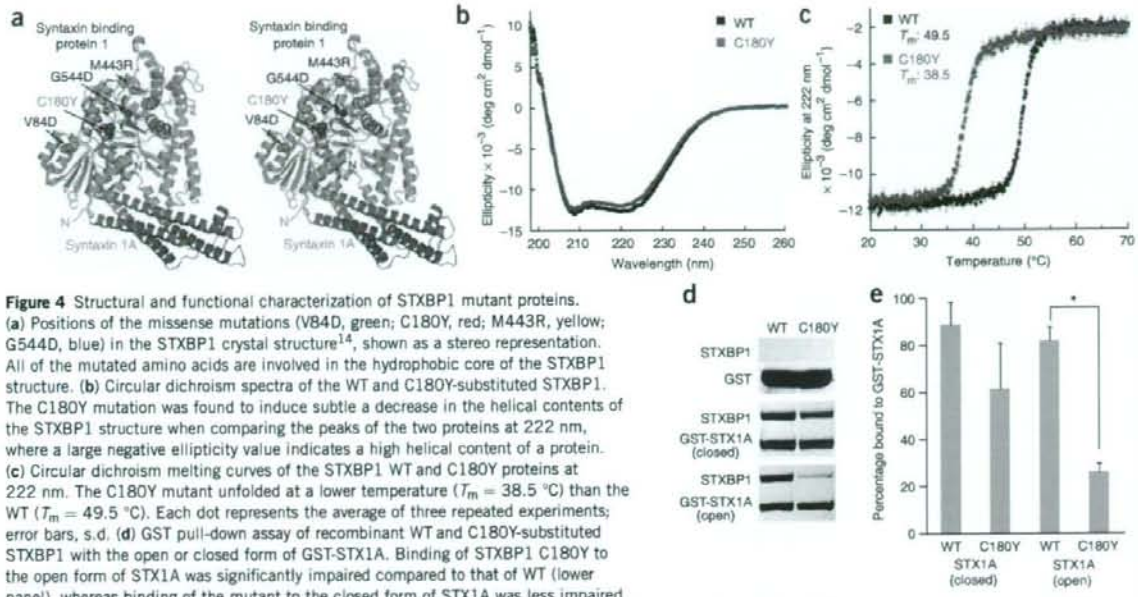

Figure 4 Structural and functional characterization of STXBP1 mutant proteins. (**a**) Positions of the missense mutations (V84D, green; C180Y, red; M443R, yellow; G544D, blue) in the STXBP1 crystal structure[14], shown as a stereo representation. All of the mutated amino acids are involved in the hydrophobic core of the STXBP1 structure. (**b**) Circular dichroism spectra of the WT and C180Y-substituted STXBP1. The C180Y mutation was found to induce subtle a decrease in the helical contents of the STXBP1 structure when comparing the peaks of the two proteins at 222 nm, where a large negative ellipticity value indicates a high helical content of a protein. (**c**) Circular dichroism melting curves of the STXBP1 WT and C180Y proteins at 222 nm. The C180Y mutant unfolded at a lower temperature (T_m = 38.5 °C) than the WT (T_m = 49.5 °C). Each dot represents the average of three repeated experiments; error bars, s.d. (**d**) GST pull-down assay of recombinant WT and C180Y-substituted STXBP1 with the open or closed form of GST-STX1A. Binding of STXBP1 C180Y to the open form of STX1A was significantly impaired compared to that of WT (lower panel), whereas binding of the mutant to the closed form of STX1A was less impaired (middle panel). In a control experiment, neither WT nor C180Y STXBP1 showed any binding to GST alone (upper panel). (**e**) Quantitative analysis of the interaction between STXBP1 and GST-STX1A based on the data shown in **d**. *P = 0.000148 by unpaired Student's t-test, two-tailed. Averages of three repeated experiments; error bars, s.d.

© 2008 Nature Publishing Group http://www.nature.com/naturegenetics

abnormalities[5,6], but we did not recognize any in the five subjects with EIEE having *STXBP1* defects. Suppression-burst pattern on the EEG has been observed in individuals with cerebral conditions disconnecting the cortex from deep structures, such as deep brain tumors, stroke with severe anoxia and barbiturate anesthesia[1,27]. Tonic seizures in EIEE have been suggested to originate from subcortical structures, especially the brainstem[5]. Notably, although normal brain architecture develops in *Stxbp1* null mice, extensive cell death of mature neurons occurs first in lower brain areas, and the lower brainstem is almost completely lost by embryonic day 18 (ref. 2). Thus, in addition to the impaired synaptic vesicle release, neuronal cell death in the brainstem might contribute to EIEE pathogenesis, although brain MRI did not show brainstem abnormalities in individuals with aberrant *STXBP1*. Delayed myelination or hypomyelination in subjects 1, 6 and 7 may also affect corticosubcortical connections.

In conclusion, we have identified heterozygous mutations of *STXBP1* at 9q34.11 in individuals with EIEE. It is noteworthy that autosomal *STXBP1* abnormalities can explain EIEE in both sexes. Understanding the abnormal synaptic vesicle release underlying EIEE may provide new insights for intractable spasms in infancy.

METHODS

Subjects. We analyzed a total of 14 Japanese individuals with EIEE. The diagnosis was made on the basis of clinical features, including early onset of tonic spasms, seizure intractability and psychomotor retardation as well as characteristic suppression-burst pattern on the EEG. Experimental protocols were approved by the Committee for Ethical Issues at Yokohama City University School of Medicine. Informed consent was obtained for all individuals included in this study in agreement with the requirements of Japanese regulations. Clinical histories of subjects with *STXBP1* aberrations are described in **Table 1** and **Supplementary Note**, except for subject 1, whose clinical information has been previously reported (as no. 2)[13].

Microarray analysis. We developed a BAC array containing 4,219 BAC clones spanning the entire human genome. We selected 5,042 BAC/PAC (phage P1-derived artificial chromosome) clones using the University of California Santa Cruz (UCSC) Genome Browser (2003 July version), with spacing at every 0.7 Mb of the human genome, and chose for arrays 4,219 clones that showed a unique FISH signal at the predicted chromosomal location. The other 822 clones were not spotted on slides, as 438 (8.7%) yielded more than one chromosomal signal by FISH and 384 (7.6%) showed a signal on a different chromosome that was probably due to contamination in our laboratory. The 4,219 clones also included 59 BAC/PAC clones previously used for a microarray targeting all chromosomal subtelomeres and critical regions for mental retardation syndromes[28]. BAC/PAC DNA was extracted using an automatic DNA extraction system PI-100 (Kurabo), amplified by two-round PCR, purified and adjusted to the final concentration >500 ng/μl, and spotted in duplicate on CodeLink activated slides (Amersham) by the ink-jet spotting method (Nihon Gaishi).

aCGH analysis was performed as described previously[29]. Briefly, after complete digestion using DpnII, subject's DNA was labeled in experiment 1 (CGH1) with Cy-5 dCTP (GE Healthcare) and control DNA was labeled with Cy-3 dCTP (GE Healthcare) using the BioPrime Array CGH Genomic Labeling System (Invitrogen). To rule out false positives, dyes were swapped in CGH2 (subject's DNA with Cy3 and control DNA with Cy5) to check whether the signal patterns obtained in CGH1 were reversed. After drying, the arrays were scanned by GenePix 4000B (Axon Instruments) and analyzed using GenePix Pro 6.0 (Axon Instruments). The signal intensity ratio between the subject's and the control DNA was calculated from the data of the single-slide experiment in each of CGH1 and CGH2, using the ratio of means formula (F635 mean – B635 median / F532 mean – B532 median, where 'F635 mean' is the mean of all the feature pixel intensities at 635 nm, 'B635 median' is the median of all the background pixel intensities at 635 nm, and 'F532 mean' and 'B532 median' are defined similarly at 532 nm) according to GenePix Pro. 6.0. The s.d. of each clone was then calculated. The signal ratio was regarded as 'abnormal' if it ranged outside ± 3 s.d. in both CGH1 and CGH2, with opposite directions.

FISH analysis. BAC/PAC DNA was labeled with SpectrumGreen-11-dUTP or SpectrumOrange-11-dUTP (Vysis) by nick translation and denatured at 70 °C for 10 min. Probe-hybridization mixtures (15 µl) were applied to chromosomes, incubated at 37 °C for 16–72 h, then washed and mounted in antifade solution (Vector) containing 4,6-diamidino-2-phenylindole (DAPI). Photographs were taken on an AxioCam MR CCD fitted to Axioplan2 fluorescence microscope (Carl Zeiss).

Mutation screening. Genomic DNA was obtained from peripheral blood leukocytes according to standard protocols. DNA for mutation screening was amplified using Genomiphi version 2 (GE Healthcare). Mutation screening of exons 1 to 20 covering the *STXBP1* coding region was performed by high resolution melt analysis. Real-time PCR and subsequent high-resolution melt analysis were performed in 12-µl mixture on RoterGene-6200 HRM (Corbett Life Science). For exons 2 to 20, the PCR mixture contained 1× ExTaq buffer, 0.2 mM each dNTP, 0.2 µM each primer, 1 µl DMSO, 1 µl LCGreen Plus (Idaho Technology) and 0.25 U ExTaqHS polymerase (Takara). For exon 1, the PCR mixture contained 1× GC buffer II, 0.4 mM each dNTP, 0.2 µM each primer, 1 µl LCGreen Plus (Idaho Technology) and 0.5 U LA Taq polymerase (Takara). PCR conditions and primer sequences are showed in **Supplementary Table 1** online. If a sample showed an aberrant melting curve pattern, the PCR product was purified with ExoSAP (USB) and sequenced for both forward and reverse strands with BigDye Terminator chemistry version 3 according to the standard protocol (Applied Biosystems). The reaction mixture was purified using Sephadex G-50 (GE Healthcare) and Multiscreen-96 (Millipore). Sequences were obtained on the ABI Genetic Analyzer 3100 (Applied Biosystems) with sequence analysis software version 5.1.1 (Applied Biosystems) and SeqScape version 2.1.1 (Applied Biosystems). All mutations were also verified on PCR products directly using genomic DNA as a template.

Parentage testing. For all families showing *de novo* mutations, we confirmed parentage by microsatellite analysis using ABI Prism linkage mapping set version 2.5, MD10 (Applied Biosystems). We chose 12 probes for screening (*D6S422, D7S493, D8S285, D9S161, D10S208, D11S987, D12S345, D16S503, D17S921, D18S53, D19S220* and *D20S196*), and considered biological parents confirmed if more than four informative markers were compatible in each family.

Expression vectors. A full-length human *STXBP1* cDNA clone (amino acids 1–594, GenBank accession number BC015749) and *STX1A* cDNA clone (amino acids 1–288, accession number BC064644) were purchased from Invitrogen. *STXBP1* and *STX1A* (amino acids 1–263, cytoplasmic domain as a closed form) cDNAs were cloned into pGEX6P-3 (GE Healthcare) to generate glutathione S-transferase (GST) fusion proteins. Site-directed mutagenesis was performed using a KOD-Plus-Mutagenesis kit (Toyobo) according to the manufacturer's protocol to generate *STXBP1* mutants including 251T>A (V84D), 539G>A (C180Y), 1328T>G (M443R) and 1631G>A (G544D). To produce an open form of STX1A, we generated L165A E166A double mutants[30] by site-directed mutagenesis using a KOD-Plus-Mutagenesis kit (Toyobo). All variant cDNAs were verified by sequencing.

Protein expression, purification and binding assay. Protein expression was performed in *Escherichia coli* BL21 (DE3). Bacteria were grown at 37 °C in Terrific Broth media with 300 µg/ml ampicillin to a density yielding an absorbance at 600 nm of 0.8, then protein expression was induced with 0.5 mM isopropyl-β-D-thiogalactoside (IPTG) at 20 °C (WT STXBP1, STX1A) or 18 °C (C180Y mutant of STXBP1) overnight. Cells were collected by centrifugation and lysed using a French press (SLM Aminco). Proteins were purified by affinity chromatography using Glutathione Sepharose High Performance (GE Healthcare). GST tags of STXBP1 were removed by digestion with human rhinovirus 3C protease at 4 °C. STXBP1 was further purified by HiTrap Q HP (GE Healthcare) and Superdex-75 (GE Healthcare) columns in a buffer containing 200 mM NaCl, 20 mM sodium phosphate buffer, pH 7.5 and 1 mM dithiothreitol (DTT).

For the GST pull-down assay to measure the binding activity of STXBP1 (WT or C180Y mutant), we prepared glutathione Sepharose 4B column beads (GE Healthcare) bound to either GST or GST-STX1A protein (closed or open form). Seven micrograms of STXBP1 (WT or C180Y mutant) proteins were incubated for 1 h at 4 °C with gentle agitation in a binding buffer containing 200 mM NaCl, 20 mM sodium phosphate buffer, pH 7.5, 1 mM DTT and 0.1% Triton X-100. The beads were collected by centrifugation and washed rapidly four times with binding buffer. The bound molecules were eluted with a buffer containing 300 mM NaCl, 20 mM sodium phosphate buffer, pH 7.5, 5 mM DTT, 1 mM EDTA and 16 mM reduced glutathione. The eluted fractions were analyzed by SDS-PAGE, and protein bands were visualized by staining with Coomassie brilliant blue. The protein bands were analyzed by quantitative densitometry using a FluorChem 8900 (Alpha Inntech). Experiments were repeated three times. The STX1A-binding activities of STXBP1 (WT or C180Y mutant) were estimated as density ratios of STXBP1 and GST-STX1A in the eluted samples. Statistical analyses were done using the unpaired Student's *t*-test (two-tailed).

Circular dichroism measurements. We measured far-UV circular dichroism spectra using a J725 spectropolarimeter (Jasco) equipped with a thermoelectric temperature control system (Peltier). All data were collected using a quartz cuvette with a path length of 1 mm and a spectral bandwidth of 1 nm. The experiments were performed in 20 mM sodium phosphate buffer, pH 7.5, containing 200 mM NaCl and 1 mM DTT. The protein concentration was 5 µM for wavelength scans and 2.5 µM for temperature scans. For wavelength scan experiments, the ellipticity was scanned from 300 to 198 nm at 4 °C. Averages of three scans were recorded. Spectra were corrected for contributions of buffer solution. The secondary structure was estimated using the Yang method[15] encoded in the software bundled with the circular dichroism instrument. For temperature scan experiments, a change of ellipticity at a wavelength of 222 nm was monitored at a scan rate of 0.75 K/min from 20 to 70 °C. T_m was calculated by fitting a sigmoid-function equation using KaleidaGraph (Synergy Software). The data from three independent experiments were averaged and the s.d. calculated.

URLs. UCSC Genome Browser, http://genome.ucsc.edu/cgi-bin/hgGateway; CLUSTALW, http://align.genome.jp/.

Accession codes. GenBank: human syntaxin binding protein 1 mRNA (*STXBP1*) isoform a, NM_003165; *STXBP1* mRNA isoform b, NM_001032221. Protein Data Bank: neuronal-Sec1-syntaxin 1a complex crystal structure, 1DN1. Gene Expression Omnibus: aCGH data have been deposited with accession code GSE10077.

Note: Supplementary information is available on the Nature Genetics website.

ACKNOWLEDGMENTS

We thank subjects and their families for their participation in this study. This work was supported by Research Grants from the Ministry of Health, Labour and Welfare (N.M.) and a Grant-in-Aid for Scientific Research on Priority Areas from the Ministry of Education, Culture, Sports, Science and Technology of Japan (N.M.).

AUTHORS CONTRIBUTIONS

H.S. and N.M. designed and directed the study and wrote the manuscript; M.K., H.O., J.T., K.U., S.K. and K. Hayasaka collected samples and provided clinical information of the subjects; T.M. performed aCGH and FISH analysis; H.S., K.N., A.N., I.O. and Y.Y. provided gene sequences of the subjects; H.S., S.-i.H., T.K. and A.F. did transfection experiments; and H.S., K. Hamada and K.O. performed protein functional and structural analyses.

Published online at http://www.nature.com/naturegenetics
Reprints and permissions information is available online at http://npg.nature.com/reprintsandpermissions

1. Ohtahara, S. *et al.* On the specific age dependent epileptic syndrome: the early-infantile epileptic encephalopathy with suppression-burst [in Japanese with English abstract]. *No To Hattatsu* **8**, 270–279 (1976).
2. Verhage, M. *et al.* Synaptic assembly of the brain in the absence of neurotransmitter secretion. *Science* **287**, 864–869 (2000).
3. Harrison, S.D., Broadie, K., van de Goor, J. & Rubin, G.M. Mutations in the Drosophila *Rop* gene suggest a function in general secretion and synaptic transmission. *Neuron* **13**, 555–566 (1994).
4. Weimer, R.M. *et al.* Defects in synaptic vesicle docking in unc-18 mutants. *Nat. Neurosci.* **6**, 1023–1030 (2003).

© 2008 Nature Publishing Group http://www.nature.com/naturegenetics

5. Djukic, A., Lado, F.A., Shinnar, S. & Moshe, S.L. Are early myoclonic encephalopathy (EME) and the Ohtahara syndrome (EIEE) independent of each other? *Epilepsy Res.* **70** (suppl. 1), S68–S76 (2006).
6. Ohtahara, S. & Yamatogi, Y. Ohtahara syndrome: with special reference to its developmental aspects for differentiating from early myoclonic encephalopathy. *Epilepsy Res.* **70**, S58–S67 (2006).
7. Kato, M., Das, S., Petras, K., Sawaishi, Y. & Dobyns, W.B. Polyalanine expansion of ARX associated with cryptogenic West syndrome. *Neurology* **61**, 267–276 (2003).
8. Kato, M. *et al.* A longer polyalanine expansion mutation in the *ARX* gene causes early infantile epileptic encephalopathy with suppression-burst pattern (Ohtahara syndrome). *Am. J. Hum. Genet.* **81**, 361–366 (2007).
9. Vissers, L.E.L.M., Veltman, J.A., van Kessel, A.G. & Brunner, H.G. Identification of disease genes by whole genome CGH arrays. *Hum. Mol. Genet.* **14**, R215–R223 (2005).
10. Feuk, L., Marshall, C.R., Wintle, R.F. & Scherer, S.W. Structural variants: changing the landscape of chromosomes and design of disease studies. *Hum. Mol. Genet.* **15**, R57–R66 (2006).
11. Garcia, E.P., Gatti, E., Butler, M., Burton, J. & De Camilli, P. A rat brain Sec1 homologue related to Rop and UNC18 interacts with syntaxin. *Proc. Natl. Acad. Sci. USA* **91**, 2003–2007 (1994).
12. Kalidas, S. *et al.* Expression of p67 (Munc-18) in adult human brain and neuroectodermal tumors of human central nervous system. *Acta Neuropathol.* **99**, 191–198 (2000).
13. Tohyama, J. *et al.* Early onset West syndrome with cerebral hypomyelination and reduced cerebral white matter. *Brain Dev.* **30**, 349–355 (2008).
14. Misura, K.M.S., Scheller, R.H. & Weis, W.I. Three-dimensional structure of the neuronal-Sec1-syntaxin 1a complex. *Nature* **404**, 355–362 (2000).
15. Yang, J.T., Wu, C.S. & Martinez, H.M. Calculation of protein conformation from circular dichroism. *Methods Enzymol.* **130**, 208–269 (1986).
16. Dulubova, I. *et al.* Munc18–1 binds directly to the neuronal SNARE complex. *Proc. Natl. Acad. Sci. USA* **104**, 2697–2702 (2007).
17. Toonen, R.F. & Verhage, M. Munc18–1 in secretion: lonely Munc joins SNARE team and takes control. *Trends Neurosci.* **30**, 564–572 (2007).
18. Rickman, C., Medine, C.N., Bergmann, A. & Duncan, R.R. Functionally and spatially distinct modes of munc18-syntaxin 1 interaction. *J. Biol. Chem.* **282**, 12097–12103 (2007).
19. Shen, J., Tareste, D.C., Paumet, F., Rothman, J.E. & Melia, T.J. Selective activation of cognate SNAREpins by Sec1/Munc18 proteins. *Cell* **128**, 183–195 (2007).
20. Weimer, R.M. & Richmond, J.E. Synaptic vesicle docking: a putative role for the Munc18/Sec1 protein family. *Curr. Top. Dev. Biol.* **65**, 83–113 (2005).
21. Sudhof, T.C. The synaptic vesicle cycle. *Annu. Rev. Neurosci.* **27**, 509–547 (2004).
22. Rizo, J. & Sudhof, T.C. Snares and Munc18 in synaptic vesicle fusion. *Nat. Rev. Neurosci.* **3**, 641–653 (2002).
23. Hata, Y., Slaughter, C.A. & Sudhof, T.C. Synaptic vesicle fusion complex contains unc-18 homologue bound to syntaxin. *Nature* **366**, 347–351 (1993).
24. Gurnett, C.A. & Hedera, P. New ideas in epilepsy genetics: novel epilepsy genes, copy number alterations, and gene regulation. *Arch. Neurol.* **64**, 324–328 (2007).
25. Garcia, C.C. *et al.* Identification of a mutation in synapsin I, a synaptic vesicle protein, in a family with epilepsy. *J. Med. Genet.* **41**, 183–186 (2004).
26. Toonen, R.F. *et al.* Munc18–1 expression levels control synapse recovery by regulating readily releasable pool size. *Proc. Natl. Acad. Sci. USA* **103**, 18332–18337 (2006).
27. Spreafico, R. *et al.* Burst suppression and impairment of neocortical ontogenesis: electroclinical and neuropathologic findings in two infants with early myoclonic encephalopathy. *Epilepsia* **34**, 800–808 (1993).
28. Harada, N. *et al.* Subtelomere specific microarray based comparative genomic hybridisation: a rapid detection system for cryptic rearrangements in idiopathic mental retardation. *J. Med. Genet.* **41**, 130–136 (2004).
29. Miyake, N. *et al.* BAC array CGH reveals genomic aberrations in idiopathic mental retardation. *Am. J. Med. Genet. A.* **140**, 205–211 (2006).
30. Dulubova, I. *et al.* A conformational switch in syntaxin during exocytosis: role of munc18. *EMBO J.* **18**, 4372–4382 (1999).

© 2008 Nature Publishing Group http://www.nature.com/naturegenetics

Journal of Neurochemistry

JOURNAL OF NEUROCHEMISTRY | 2008 | 107 | 918–927

doi: 10.1111/j.1471-4159.2008.05666.x

Neuroprotective effect of sonic hedgehog up-regulated in Schwann cells following sciatic nerve injury

Manabu Hashimoto,*[,1] Kunihiro Ishii,†[,1] Yasuko Nakamura,* Kazuhiko Watabe,‡ Shinichi Kohsaka* and Chihiro Akazawa*[,†]

*Department of Neurochemistry, National Institute of Neuroscience, NCNP, Kodaira, Tokyo, Japan

†Department of Biochemistry and Biophysics, Graduate School of Health and Sciences, Tokyo Medical and Dental University, Bunkyo, Tokyo, Japan

‡Tokyo Metropolitan Institute for Neuroscience, Fuchu, Tokyo, Japan

Abstract

The physiological roles of sonic hedgehog (Shh) have been intensively characterized in development of various organs. However, their functions in adult tissues have not been fully elucidated. We investigated the expression and the potential function of Shh in crush-injured adult rat sciatic nerves. The Shh expression was up-regulated in Schwann cells adjacent to the injured site. The time-course analyses of various neurotrophic factors revealed the up-regulation of Shh mRNA followed by that of brain-derived neurotrophic factor (BDNF) mRNA. The continuous administration of cyclopamine, a hedgehog signal inhibitor, to the injured site suppressed the increase of BDNF expression and deteriorated the survival of motor neurons in lumbar spinal cord. Treatment of exogenous Shh in cultured Schwann cells enhanced the BDNF expression. The BDNF promoter activity (exon I and II) was increased in IMS32 cells co-transfected with Shh and its receptor Smoothened. These findings imply that the up-regulated expression of Shh in Schwann cells may play an important role in injured motor neurons through the induction of BDNF.

Keywords: brain-derived neurotrophic factor, nerve injury, real-time polymerase chain reaction, Schwann cells, sciatic nerve, sonic hedgehog.

J. Neurochem. (2008) **107**, 918–927.

Nerve injury triggers a number of responses in many cells around the injury site and influences the fate of injured neurons, for example, neuronal survival or axonal regeneration (Loers and Schachner 2007). The regulation of gene expression is one of the major issues, because its function after injury is critical to understand the mechanism of nerve regeneration. Our previous studies demonstrated that the sonic hedgehog (Shh) expression was up-regulated in facial motor neurons after facial nerve axotomy, and Shh might promote survival of injured motor neurons (Akazawa *et al.* 2004). To further investigate the neuroprotective effects of Shh, here we used a crush-injury of sciatic nerve and investigated the local expression of Shh after nerve injury.

Shh has been intensively characterized in the developmental stages of various organs, including motor neuron differentiation (Richardson *et al.* 1997; Briscoe *et al.* 1999; Soula *et al.* 2001), and limb development (te Welscher *et al.* 2002). In adult stage, it has been reported that Shh is involved in the formation of various tumors (Berman *et al.* 2003; Riobo *et al.* 2006), however, the other roles are little known. Shh functions through binding to the 12-transmembrane receptor patched-1 (Ptc1) (Stone *et al.* 1996). Without Shh, Ptc1 inhibits the intracellular signaling of the 7-transmembrane receptor Smoothened (Smo) (Xie *et al.* 1998). Binding of Shh to Ptc1 releases the inhibition of Smo and subsequently activates the transcriptional factor Gli1 (Hahn *et al.* 1999).

Various lines of evidence indicate that neurotrophic factors, including brain-derived neurotrophic factor (BDNF), neurotrophin (NT)-3, NT-4/5, ciliary neurotrophic factor, and

Received March 31, 2008; revised manuscript received July 29, 2008; accepted August 12, 2008.

Address correspondence and reprint requests to Shinichi Kohsaka, Department of Neurochemistry, National Institute of Neuroscience, NCNP, Japan, Ogawahigashi 4-1-1, Kodaira, Tokyo 187-8502, Japan. E-mail: kohsaka@ncnp.go.jp

[1]These two authors contribute equally in this work.

Abbreviations used: BDNF, brain-derived neurotrophic factor; GDNF, glial cell line-derived neurotrophic factor; HBC, 2-hydroxypropyl)-β-cyclodextrin; PBS, phosphate-buffered saline.

© 2008 The Authors
Journal Compilation © 2008 International Society for Neurochemistry,

glial cell line-derived neurotrophic factor (GDNF), have been shown to prevent the neuronal cell death after axotomy of motor neurons (Funakoshi *et al.* 1993; Friedman *et al.* 1995; Houenou *et al.* 1996; Aszmann *et al.* 2002; Yamada *et al.* 2004). In this study, we found that the expression profile of Shh, GDNF, and BDNF seems to be mutually linked, and tried to sort out the regulation among these molecules. We hypothesized that Shh may play a neuroprotective role at least in part through BDNF. To elucidate its mechanism, the expression of Shh, BDNF, and GDNF after sciatic nerve injury was first investigated. Next, we examined the effect of Shh signaling inhibition on the expression of neurotrophic factors.

Materials and methods

Animals and surgery

All procedures in this study were approved by the ethical committee upon animal experiments of the National Institute of Neuroscience, NCNP, Japan, that was consistent with US Federal guidelines. Adult Wistar rats (200–250 g) were housed under 12 : 12 hour light/dark cycle, with food and water available ad labium. Under deep anesthesia using ether, the sciatic nerves were crushed at the distal obturator tendon using forceps by which the grade of pressure was adjusted. Cyclopamine (Biomol, International, Plymouth, UK) was continuously administered to the injury site of sciatic nerve using osmotic pumps (Durect, Cupertino, CA, USA) with a delivery rate of 1 μL/h. Pumps containing 500 μg/mL cyclopamine dissolved in 45% [2-hydroxypropyl)-β-cyclodextrin (HBC)] (Sigma, St Louis, MO, USA) were implanted in the right side of rat. The contents of pumps were continuously delivered to right injury site through a vinyl catheter tube for 1 week. Likewise, pumps containing 45% HBC (vehicle) were implanted in the left side, and the contents were injected to left injury site.

Reverse transcription and real-time polymerase chain reaction

The proximal or distal segment (10 mm length) among the crushed-site was respectively collected. Total RNA was prepared from the pooled nerve segments by using Isogen (Nippon Gene, Tokyo, Japan), which is basically composed of guanidine isothiocyanate. The reverse transcription was performed with a SMART cDNA Synthesis Kit (Clontech, Palo Alto, CA, USA) according to the instructions. In brief, 500 ng of RNA was denatured for 2 min at 70°C, and reverse-transcribed with MMLV-Reverse Transcriptase for 1 h at 42°C. Afterwards, the transcriptase was inactivated by heating for 7 min at 72°C. The real-time polymerase chain reaction (PCR) was employed for the relative quantification of Shh, Gli1, BDNF, GDNF, Ptc1, and Smo transcripts for a glyceraldehyde-3-phosphate dehydrogenase (GADPH) as a control. The primer sequences were listed in Supporting information Table S1. The Light Cycler Instrument (Roche Diagnostics, Indianapolis, IN, USA) and the SYBR Premix Ex Taq (Takara Bio Europe S.A., Gennevilliers, France) were used. This 'hot start' reaction mix contains Takara Ex TaqHS DNA polymerase, dNTP mix, and the fluorescent dye SYBR Green I for real-time detection of double-stranded DNA. Relative expression of RT-PCR products was determined using the $\Delta\Delta C_t$ method (Winer *et al.* 1999): fold induction = $2^{-\Delta\Delta C_t}$; where C_t is the threshold cycle, i.e., the cycle number at which the sample's relative fluorescence rises above the background fluorescence and $\Delta\Delta C_t$ = [C_t gene of interest (unknown sample) – C_t GAPDH (unknown sample)] – [C_t gene of interest (calibrator sample) – C_tGAPDH (calibrator sample)]. One of the control samples was chosen as the calibrator sample and used in each PCR. Each sample was run in triplicate and the mean C_t was used in the $\Delta\Delta C_t$ equation.

In situ hybridization

Double labeled *in situ* hybridization was carried with a slight modification described elsewhere (Akazawa *et al.* 2004). In short, fresh-frozen sections of 14 μm thickness were prepared in a cryostat and thaw-mounted onto slide glasses (Superfrost Plus, Fisher Scientific, Pittsburgh, PA, USA), following briefly dried and stored in −80°C. The anti-sense riboprobes were synthesized by transcription using either T7 RNA-polymease (Roch Boehringer, Mannheim, Germany) in the presence of digoxigenin-UTP (Roch Boehringer) for Shh or fluorescein-UTP (Roch Boehringer) for myelin protein P0 (P0) for 30 min at 37°C. The either digoxigenin- or fluorescein-labeled RNA probe was column-purified and reconstituted in TE (10 mM Tris–HCl, pH 7.4, 5 mM EDTA) at the concentration of 1 μg/mL. Before the hybridization experiments, sections were fixed in 4% paraformaldehyde in 0.1 M phosphate-buffered saline (PBS) for 20 min and washed twice in PBS, and subjected to the overnight hybridization at 65°C in a mixture (50% formamide, 10 mM PBS, 20 mM Tris–HCl, pH 7.4, 5 mM EDTA, 10% dextran sulfate, 1× Denhardt's reagents, 0.2% sodium lauryl sarcosine, 500 μg/mL t-RNA, 200 μg/mL sonicated single strand-DNA) containing two labeled probes (0.1 μg/μL hybridization mixture for each probe). After hybridization, sections were washed in 10 mM dithiothreitol in 5× sodium chloride/sodium citrate at 55°C. After three-series of washing, sections were treated with the avidin/biotin blocking kit (Vector, Burlingame, CA, USA) and then incubated for 1 h in a mix of alkaline phosphatase (AP)-conjugated rabbit anti-digoxigenin antibody (1 : 500 dilution, Roche Diagnostics) and mouse anti-FITC antibody (1 : 500, Roche Diagnostics). Subsequently, sections were incubated for 1 h in biotinylated anti-mouse secondary antibody (1 : 500, Jackson Laboratory, West Grove, PA, USA), which was followed by several washes in Tris-NaCl-Tween (0.1 M Tris, pH 7.5, 0.15 M NaCl, 0.05% Tween-20) and a incubation for 30 min in avidin-conjugated horseradish peroxidase (1 : 500, Vector) in Tris-NaCl-Tween containing 0.5% blocking reagent (Vector). The sequential chromogenic reaction was performed using Magenta-phos-*p*-tol (Thermo Fisher Scientific, Walthman, MA, USA) as a substrate for AP and HsitoMark TrueBlue (KPL, Inc. Gaithersburg, MD, USA) as a substrate for horseradish peroxidase.

Immunohistochemical study

One week after the sciatic nerve crush, animals were cardioperfused with cold 4% paraformaldehyde solution prepared in 0.1 M PBS, pH 7.3 (the fixative). The sciatic nerve was frozen in embedding compound (Tissue-Tec; Miles, Elkhart, IN, USA). Longitudinal sections of 20-μm thickness were cut with a cryostat (Leica, Deerfield, IL, USA) and thawed on cover glasses coated by (3-aminopropyl) triethoxysilane. Then, they were rinsed in 0.1 M Tris–HCl buffer, pH 7.6, containing 0.3% Triton X-100 (TT buffer)

© 2008 The Authors
Journal Compilation © 2008 International Society for Neurochemistry,